JOURNAL OF Materials CHEMISTRY

Structural, magnetic, electrical and optical characterization of systems built from $[M([9]aneN_3)_2]^{2+}$ (M = Cu^{II} or Ni^{II}) and TCNQ or $TCNQF_4$

M. Teresa Azcondo,*†[a] Loreto Ballester,*[b] Stephane Golhen,[c] Angel Gutierrez,[b] Lahcene Ouahab,[c] Slav Yartsev[d] and Pierre Delhaes*[a]

[a]*Centre de Recherche Paul Pascal, CNRS, Av. Dr. Schweitzer, 33600 Pessac, France*
[b]*Departamento de Química Inorgánica, Facultad de Ciencias Químicas, Universidad Complutense, 28040 Madrid, Spain*
[c]*Laboratoire de Chimie du Solide et Inorganique Moleculaire, Av. du Général Leclerc, 35042 Rennes, France*
[d]*Centro de Fisica, IVIC, Apartado 21827, Caracas 1020-A, Venezuela*

Received 30th September 1998, Accepted 1st March 1999

Three different supramolecular architectures corresponding to $[M([9]aneN_3)_2](TCNQ)_2$, (M = Ni^{II} **1** or Cu^{II} **2**, $[9]aneN_3$ = 1,4,7-triazacyclononane, TCNQ = 7,7,8,8-tetracyanoquinodimethane), $[Cu([9]aneN_3)_2](TCNQ)_3$ **3** and $[Cu([9]aneN_3)_2](TCNQF_4)_2$, **4** ($TCNQF_4$ = 2,3,5,6-tetrafluoro-7,7,8,8,-tetracyanoquinodimethane), have been prepared and crystallographically characterized: **1**, triclinic, $P\bar{1}$, a = 8.6488(9), b = 8.919(3), c = 11.316(2) Å, α = 82.06(2), β = 74.331(10), γ = 85.71(2)°, Z = 1; **2**, triclinic, $P\bar{1}$, a = 8.6806(11), b = 8.915(5), c = 11.348(2) Å, α = 82.03(3), β = 74.109(14), γ = 84.95(2)°, Z = 1; **3**, triclinic, $P\bar{1}$, a = 8.350(2), b = 9.884(4), c = 14.369(4) Å, α = 74.10(2), β = 89.01(2), γ = 69.11(2)°, Z = 1; **4**, triclinic, $P\bar{1}$, a = 15.476(5), b = 16.146(4), c = 16.441(4) Å, α = 77.15(2), β = 78.04(3), γ = 85.43(3)°, Z = 2. Compounds **1** and **2** are formed by dimeric $(TCNQ)_2^{2-}$ units and **4** by three different dimeric $(TCNQF_4)_2^{2-}$ units. Compound **3** is formed by isolated $[Cu([9]aneN_3)_2]^{2+}$ groups and trimeric $(TCNQ)_3^{2-}$ units. The electrical, optical and magnetic properties of the four new compounds have been interpreted on the basis of their supramolecular architectures.

Introduction

In the field of molecular networks containing organic radicals, macroscopic properties such as magnetic order or electrical conductivity can be produced when the appropriate supramolecular arrangement is achieved.[1] On this basis, when paramagnetic metallic centers are integrated within organic radicals as building blocks in molecular networks, 'hybrid' materials combining the properties of the organic and inorganic components can be formed.[2]

Special attention has been given to the assemblage of organonitrile radical complexes with copper and nickel complexes because of their rich possibilities of interaction. The initial approach was directed to study donor–acceptor interactions between planar copper and nickel complexes with π electron density such as Schiff bases or porphyrin derivatives and 7,7,8,8-tetracyanoquinodimethane (TCNQ) with formation of integrated systems.[3] When complexes with a coordinatively saturated metal such as $[Cu(phen)_3]^{2+}$ or $[Ni(dien)_2]^{2+}$ are used, new compounds, such as $[Cu(phen)_3](TCNQ)_2$ and $[Ni(dien)_2](TCNQ)_2$, without direct bonding interactions between the metal and TCNQ are formed.[4]

In recent years, we have developed several new synthetic strategies in order to obtain different supramolecular architectures by controlling several factors of the transition metal fragments.[5] From these strategies, we have obtained hybrid systems with or without σ-bonded TCNQ[6] and with different degrees of electronic delocalization in the TCNQ stacks.[7]

In comparison to the TCNQ systems, the corresponding compounds with 2,3,5,6-tetrafluoro-7,7,8,8-tetracyanoquinodimethane ($TCNQF_4$) are very scarce and only metallocene derivatives have been described.[8] We report here the effect of using $TCNQF_4$ instead of TCNQ in systems containing $[Cu([9]aneN_3)_2]^{2+}$ ($[9]aneN_3$ = 1,4,7-triazacyclononane) on their supramolecular architectures and associated properties.

Experimental

All the reactions were carried out under oxygen free nitrogen. The starting materials, LiTCNQ, $LiTCNQF_4$, $Et_3HN(TCNQ)_2$[9] and $[M([9]aneN_3)_2]X_2$[10] (M = Ni, X = Cl^-; M = Cu, X = ClO_4^-, $[9]aneN_3$ = 1,4,7-triazacyclononane) were obtained by published methods. All the starting materials were checked by elemental analyses. The synthesized TCNQ and $TCNQF_4$ compounds were obtained by metathesis reactions from the parent chloride or perchlorate (Fig. 1).

CAUTION: Perchlorate salts are potentially explosive and should be used in small amounts and handled with care.

Complexes **1** and **2** were obtained by addition of a solution of LiTCNQ in methanol to a stirred solution of $[M([9]aneN_3)_2]X_2$ (M = Ni, X = Cl^-; M = Cu, X = ClO_4^-) in methanol–water (1 : 2) with a 1 : 2 molar ratio of metal complex to TCNQ. The resulting solutions were stirred, and the deep blue solids that formed were filtered off, washed with methanol and diethyl ether and dried under vacuum (Found: C, 59.73; H, 5.25; N, 27.02. Calc. for $C_{36}H_{38}N_{14}Ni$ **1**: C, 59.58; H, 5.24; N, 27.03. Found: C, 59.45; H, 5.32; N, 27.09. Calc. for $C_{36}H_{38}N_{14}Cu$ **2**: C, 59.18; H, 5.21; N, 26.85%).

Complex **3** was synthesized by addition of a solution of 0.57 mmol of $Et_3HN(TCNQ)_2$ in acetonitrile to a stirred solution of 0.38 mmol of $[Cu([9]aneN_3)_2](ClO_4)_2$ in methanol–water (1 : 2). After 1 h of stirring, a dark blue microcrystalline solid appeared. The solid was filtered off, washed with water, methanol and diethyl ether, and dried under vacuum (Found: C, 61.95; H, 4.66; N, 27.31. Calc. for $C_{48}H_{42}N_{18}Cu$

†Present address: Dra. M. T. Azcondo, Departamento de Química Inorgánica, Facultad de Ciencias Químicas, Universidad Complutense, 28040-Madrid, Spain. E-mail: mayteaz@eucmax.sim.ucm.es.

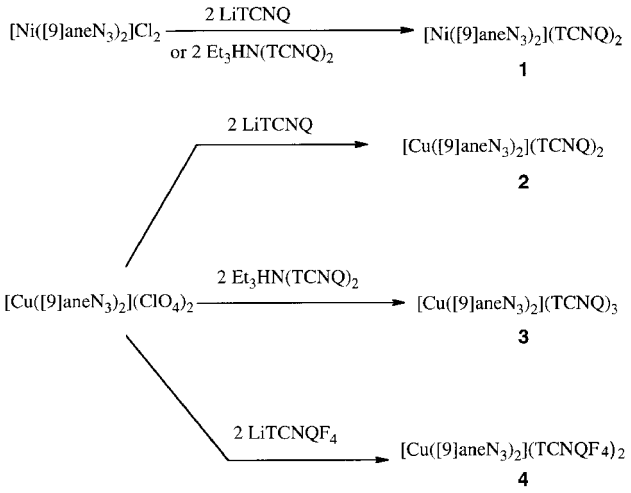

Fig. 1 Scheme of the chemical reactions.

3: C, 61.66; H, 4.50; N, 26.98%). Similar reactions with $[Ni([9]aneN_3)_2]Cl_2$ only afforded compound **1**.

Derivative **4** was obtained by the reaction of a solution of 5.65×10^{-2} mmol of $LiTCNQF_4$ in methanol which was added to a stirred solution of 2.83×10^{-2} mmol of $[Cu([9]aneN_3)_2](ClO_4)_2$ in methanol–water (1:2). After 2 h of stirring, a deep blue microcrystalline solid was filtered off, washed with water, methanol and diethyl ether and dried under vacuum.

To prepare single crystals, we used a slow diffusion of reactant solutions and good quality crystals of the four compounds were obtained.

All the compounds are dark blue and only slightly soluble in polar solvents such as acetonitrile or DMSO, and their solutions rapidly decompose in the air.

X-Ray crystal structures

Each single crystal was mounted on an Enraf Nonius CAD 4 diffractometer with graphite monochromated Mo-Kα radiation ($\lambda = 0.71073$ Å). All crystal data are summarized in Table 1. Full crystallographic details, excluding structure factors, have been deposited at the Cambridge Crystallographic Data Centre (CCDC). See Information for Authors, 1999, Issue 1. Any request to the CCDC for this material should quote the full literature citation and the reference number 1145/146. See http://www.rsc.org/suppdata/jm/1999/1237/, for crystallographic files in .cif format.

The crystal structures of **1** and **2** can be described as formed by cationic $[M([9]aneN_3)_2]^{2+}$ and dimeric $(TCNQ)_2^{2-}$ units. The atom labeling of the molecular units is shown in Fig. 2 and bond lengths and angles are listed in Table 2. The tridentate macrocycles are coordinated facially to the metal centers, which show octahedral coordination with different degrees of distortion. The nickel–nitrogen distances are in the range 2.099(3)–2.130(3) Å as is usual in octahedral nickel(II) complexes.[11] The copper–nitrogen distances are 2.038(3), 2.155(3) and 2.274(3) Å, also in the range usually found for related elongated rhombic octahedral stereochemistry.[12]

The two TCNQ molecules in the unit cell are symmetry related and are uncoordinated to the metal. The interatomic distances are characteristic of the radical anion $TCNQ^{\bullet -}$.[13] The two symmetric TCNQ molecules overlap in the ring over ring mode, forming dimeric $(TCNQ)_2^{2-}$ dianions. The shortest intradimer distance is 3.266(5) and 3.258(4) Å for the Ni^{II} and Cu^{II} derivatives, respectively, both of which lie in the usual range for uncoordinated TCNQ dimers.[4] The $(TCNQ)_2^{2-}$ units are parallel with respect to the apical position of the small macrocyclic N-donor. The shortest distance between dimers is 3.680(6) for the Ni^{II} derivative and 3.725(5) Å for the Cu^{II} one (Fig. 3). These distances are greater that the sum of the Van der Waals radii of carbon and nitrogen and, thus indicate that no interaction occurs between neighbouring $(TCNQ)_2^{2-}$ dimers.

Table 1 Crystal and refinement data for compounds **1**–**4**

Compound	$[Ni([9]aneN_3)_2](TCNQ)_2$ **1**	$[Cu([9]aneN_3)_2](TCNQ)_2$ **2**	$[Cu([9]aneN_3)_2](TCNQ)_3$ **3**	$[Cu([9]aneN_3)_2](TCNQF_4)_2$ **4**
Formula	$C_{36}H_{38}N_{14}Ni$	$C_{36}H_{38}CuN_{14}$	$C_{48}H_{42}CuN_{18}$	$C_{72}H_{60}Cu_2F_{16}N_{28}\cdot 3H_2O$
M	725.51	730.34	934.54	1802.61
Crystal system	Triclinic	Triclinic	Triclinic	Triclinic
Space group	$P\bar{1}$	$P\bar{1}$	$P\bar{1}$	$P\bar{1}$
a/Å	8.6488(9)	8.6806(11)	8.350(2)	15.476(5)
b/Å	8.919(3)	8.915(5)	9.884(4)	16.146(4)
c/Å	11.316(2)	11.348(2)	14.369(4)	16.441(4)
α/°	82.06(2)	82.03(3)	74.10(2)	77.15(2)
β/°	74.331(10)	74.109(14)	89.01(2)	78.04(3)
γ/°	85.71(2)	84.95(2)	69.11(2)	85.43(3)
V/Å^3	831.8(3)	835.3(5)	1061.2(6)	3916(2)
Z	1	1	1	2
D_c/g cm^{-3}	1.448	1.452	1.462	1.532
Radiation (λ/Å)	Mo-Kα(0.71073)	Mo-Kα(0.71073)	Mo-Kα(0.71073)	Mo-Kα(0.71073)
T/K	293(2)	293(2)	293(2)	293(2)
θ range/°	1.88–26.96	1.88–26.97	1.48–26.97	1.29–24.99
μ(Mo-Kα)/mm^{-1}	0.635	0.705	0.576	0.649
Collected reflections	3876	3873	4871	13723
Independent reflections (R_{int})	3631(0.0145)	3630(0.0136)	4546(0.0090)	13197(0.0346)
Data/parameters	3631/308	3630/308	4546/388	13192/1206
Absorption correction	ψ-Scan		ψ-Scan	
Transmission (max, min)	0.998661, 0.962918		0.998780, 0.908442	
R indices [$I > 2\sigma(I)$] (on F^2)[a]	$R_1 = 0.0551$, $wR_2 = 0.1423$	$R_1 = 0.0433$, $wR_2 = 0.1135$	$R_1 = 0.0311$, $wR_2 = 0.0829$	$R_1 = 0.0560$, $wR_2 = 0.1039$
S (on F^2)	1.058	1.005	1.055	1.030
$\Delta\rho$/e Å^{-3} (max, min)	1.304, −0.431	0.953, −0.321	0.270, −0.476	0.595, −0.521

[a] $R_1 = \sum(|F_o| - |F_c|)^2 / \sum F_o^2$, $wR_2 = (\sum[w(F_o^2 - F_c^2)^2] / \sum[w(F_o^2)^2])^{1/2}$.

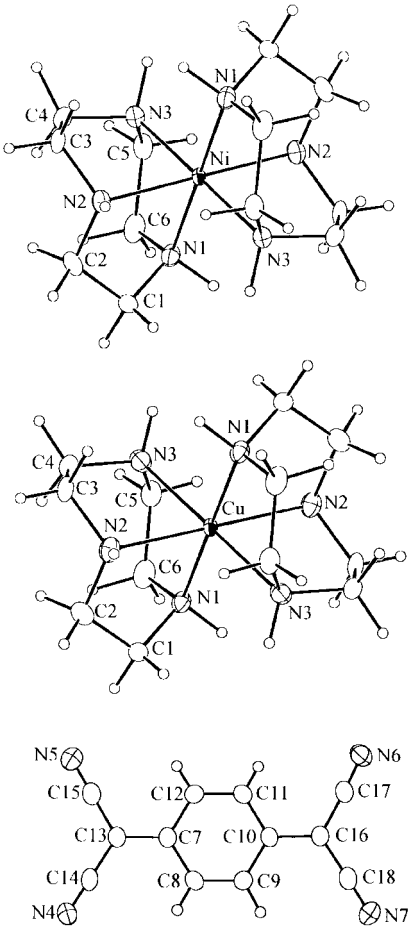

Fig. 2 Atom labeling of the molecular units of $[M([9]aneN_3)_2](TCNQ)_2$ (M = Ni, **1** Cu **2**).

Compound **3** presents a unit cell consisting of a copper fragment and three TCNQ molecules: two TCNQ molecules of type A and a third TCNQ molecule of type B. The atom labeling is shown in Fig. 4 and bond lengths and angles are listed in Table 3. The copper atom in the molecular unit is coordinated to six nitrogens of the two macrocyclic ligands. The copper environment is a tetragonally elongated octahedron with copper–nitrogen bond distances of 2.051(2), 2.054(2) and 2.382(2) Å. These distances are different from the copper environment in $[Cu([9]aneN_3)_2](TCNQ)_2$, prob-

Table 2 Selected bond distances (Å) and angles (°) for $[Ni([9]aneN_3)_2](TCNQ)_2$ **1** and $[Cu([9]aneN_3)_2](TCNQ)_2$ **2**

Cu–N1	2.038(3)	Ni–N1	2.099(3)
Cu–N2	2.155(3)	Ni–N2	2.127(3)
Cu–N3	2.274(3)	Ni–N3	2.130(3)
N4–C14	1.148(4)	N4–C14	1.139(5)
N5–C15	1.146(4)	N5–C15	1.141(5)
N6–C17	1.149(4)	N6–C17	1.147(5)
N7–C18	1.142(4)	N7–C18	1.141(5)
C7–C12	1.413(4)	C7–C12	1.412(5)
C7–C8	1.421(4)	C7–C8	1.418(5)
C7–C13	1.424(4)	C7–C13	1.423(5)
C8–C9	1.367(4)	C8–C9	1.359(5)
C9–C10	1.419(4)	C9–C10	1.422(5)
C10–C11	1.415(4)	C10–C11	1.413(5)
C10–C16	1.417(4)	C10–C16	1.420(5)
C11–C12	1.366(4)	C11–C12	1.368(5)
C13–C14	1.414(4)	C13–C14	1.412(5)
C13–C15	1.418(4)	C13–C15	1.418(5)
C16–C17	1.413(4)	C16–C17	1.412(5)
C16–C18	1.421(4)	C16–C18	1.415(5)
N1–Cu–N2	82.70(10)	N1–Ni–N2	82.53(13)
N1–Cu–N3	81.10(10)	N1–Ni–N3	81.91(10)

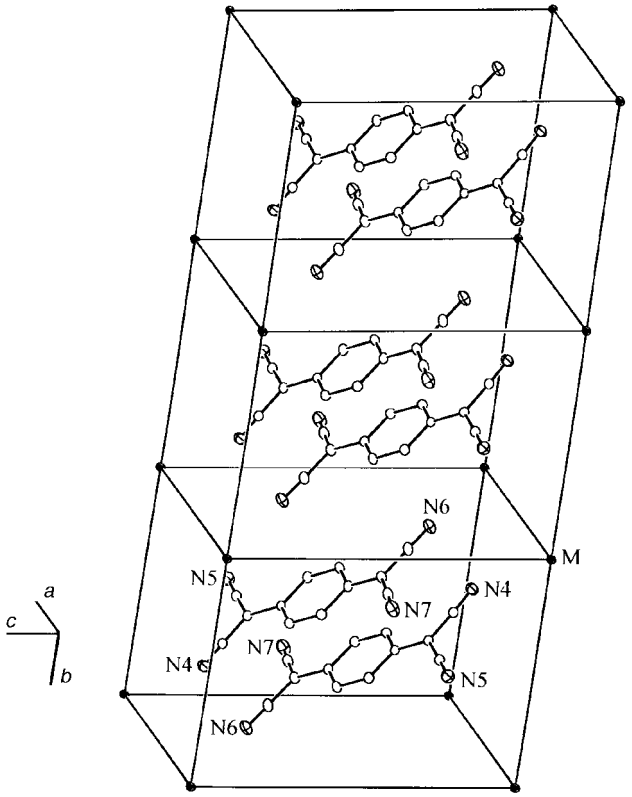

Fig. 3 Stacking of dimeric $(TCNQ)_2^{2-}$ anions in $[M([9]aneN_3)_2](TCNQ)_2$ (M = Ni **1** or Cu **2**).

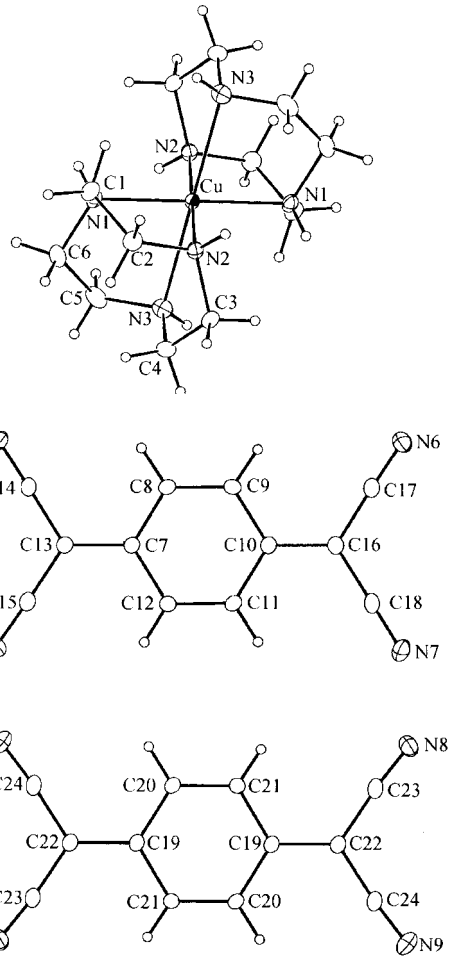

Fig. 4 Atom labeling of the molecular unit of $[Cu([9]aneN_3)_2](TCNQ)_3$ **3**.

Table 3 Selected bond distances (Å) and angles (°) for $[Cu([9]aneN_3)_2](TCNQ)_3$ **3**

Cu–N1	2.051(2)	C13–C14	1.427(2)
Cu–N2	2.054(2)	C13–C15	1.421(2)
Cu–N3	2.382(2)	C16–C17	1.423(2)
N4–C14	1.139(2)	C16–C18	1.422(2)
N5–C15	1.144(2)	N9–C24	1.142(2)
N6–C17	1.144(3)	C19–C22	1.406(2)
N7–C18	1.145(3)	C19–C20	1.421(2)
C7–C12	1.430(2)	C19–C21	1.427(2)
C7–C8	1.432(2)	C22–C23	1.414(2)
C7–C13	1.395(2)	C22–C24	1.425(2)
C8–C9	1.351(2)	N8–C23	1.423(2)
C9–C10	1.430(2)		
C10–C11	1.424(2)	N1–Cu–N2	83.88(6)
C10–C16	1.399(2)	N1–Cu–N3	79.67(6)
C11–C12	1.355(2)	N2–Cu–N3	78.76(6)

ably due to the entry of a B-type TCNQ into the composition. The three TCNQ groups interact by hydrogen bonding with amino groups of the $[Cu([9]aneN_3)_2]^{2+}$ moiety. The A- and B-type TCNQ molecules are trimerized in the structure, overlapping with the classical π–π interactions of TCNQ in the solid state. The sequence of the ABA TCNQ trimers is repeated and creates infinite parallel chains oriented along the *b* crystal axis. The π–π overlapping inside the ABA trimer is of the ring–external bond type between the A and B molecules, with a shortest intramolecular distance of 3.137(3) Å. The π–π overlapping between the two A groups of neighboring trimers is also of the ring–external bond type with a shortest distance of 3.374(3) Å. The $[Cu([9]aneN_3)_2]^{2+}$ ions also form parallel stacks in the same crystal direction and they are situated between the TCNQ chains (Fig. 5). The data on the bond lengths in the TCNQ molecules of **3** show that the non-central molecules A in the ABA trimer are not symmetrical. Using the empirical relations[13] between the bond lengths in the TCNQ molecule and its charge state, we obtain the following charge distribution in the A molecule: 0.31 e in the half of the TCNQ molecule neighboring the counter-ion and 0.25 e in the other half. The centrosymmetrical molecule B has 0.8 e charge. The total charge on the ABA trimer estimated in this manner is 1.9 ± 0.2 e as expected for neutralization of the dication $[Cu([9]aneN_3)_2]^{2+}$.

The crystal structure of derivative **4** presents a triclinic unit cell consisting of a two copper bimacrocyclic moieties and four $TCNQF_4$ groups. Molecular unit labeling is shown in Fig. 6 and bond lengths and angles are listed in Table 4. The Cu1–N bond distances are 2.167(6), 2.199(6), 2.057(5),

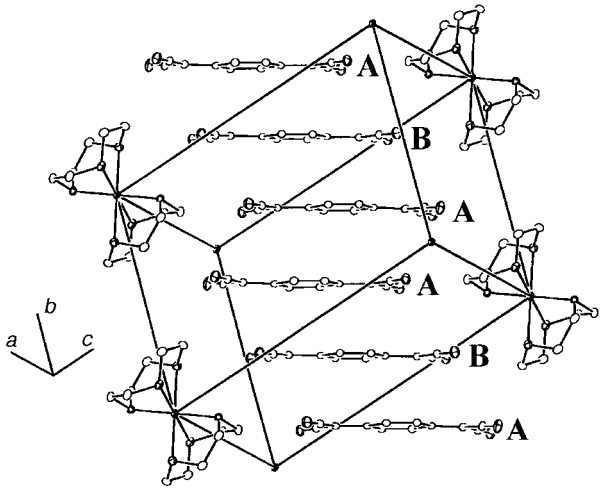

Fig. 5 Stacking of the $(TCNQ)_3^{2-}$ trimers in $[Cu([9]aneN_3)_2](TCNQ)_3$ **3**. Four of the metallic cationic units located at the cell corners are omitted for clarity.

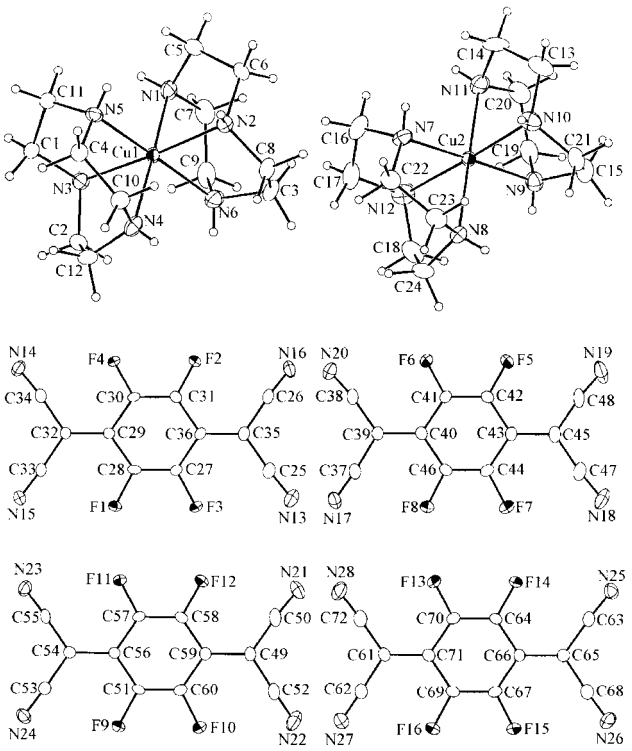

Fig. 6 Atom labeling of the molecular unit of $[Cu([9]aneN_3)_2](TCNQF_4)_2$ **4**.

2.194(7), 2.051(5) and 2.162(6) Å while the Cu2–N bond distances are 2.048(6), 2.190(7), 2.149(7), 2.062(6), 2.138(6) and 2.231(6) Å. The tridentate macrocycles are coordinated facially to the copper(II) centers, which involve an elongated rhombic octahedral stereochemistry. It is noted that owing to the steric constraints of the nine membered ring of the ligands a trigonal distortion of the CuN_6 polyhedron is also apparent, the N–Cu–N bond angles within each coordinated triamine are significantly smaller than 90° whereas N–Cu–N angles of mutually *cis* nitrogen atoms of different ligands are larger than 90°.[12] There are three different dimeric $(TCNQF_4)_2^{2-}$ units, AA, BB, and almost orthogonal CD, in the structure. The interatomic distances are characteristic of the radical anion $TCNQF_4^{\bullet -}$. The two dimeric dianions $(TCNQF_4)_2^{2-}$ (AA and BB) overlap in the ring over ring mode, the shortest intradimer distances in AA and BB are 3.209(8) and 3.278(7) Å, respectively. The dimeric anions AA and BB are stacked in the crystal forming 1-D chains of sequence ···AA BB AA BB···, the AB overlapping shows a shortest distance of 3.399(7) Å but the overlapping mode is different to those discussed above, since the longitudinal axis of type-B $TCNQF_4$ is rotated by an angle of 23° with respect to type-A $TCNQF_4$. The third dimer of $TCNQF_4^{\bullet -}$ (CD) is located between the two metallic centers Cu(1) and Cu(2). The type-C and -D $TCNQF_4^{\bullet -}$ units overlap in the ring-over-ring mode and the longitudinal axis of the type-C $TCNQF_4$ is rotated 11° with respect to the type-D $TCNQF_4$ with a shortest distance of 3.210 Å. Two type-D $TCNQF_4$ units also overlap each other, with an overlapping of the external bond–external bond type and a shortest distance of 3.335 Å.

Electrical conductivity

The conductivities of the solid state powders of compounds **1** and **2** have been measured at room temperature and they behave as insulators ($\sigma < 10^{-7}$ S cm^{-1}). The dc resistivity of single crystals of **3** and **4**, with dimensions $6 \times 1.8 \times 1$ mm and $0.22 \times 0.06 \times 0.05$ mm respectively, have been measured by the two-probe method using silver paint and 25 μm gold wires.

Table 4 Selected bond distances (Å) and angles (°) for $[Cu([9]aneN_3)_2](TCNQF_4)_2$ **4**

Cu1–N2	2.051(5)	C27–C36	1.411(8)	C43–C44	1.418(8)	C57–C58	1.359(8)
Cu1–N3	2.058(5)	C28–C29	1.424(7)	C44–C46	1.342(8)	C58–C59	1.392(8)
Cu1–N5	2.162(6)	C29–C32	1.400(7)	C45–C48	1.432(10)	C59–C60	1.411(8)
Cu1–N1	2.167(6)	C29–C30	1.418(7)	C45–C47	1.436(10)	F13–C70	1.346(6)
Cu1–N4	2.194(7)	C30–C31	1.349(7)	C47–N18	1.134(8)	F14–C64	1.344(6)
Cu1–N6	2.199(6)	C31–C36	1.414(7)	C48–N19	1.128(9)	F15–C67	1.337(6)
Cu2–N9	2.048(6)	C32–C33	1.422(8)	F9–C51	1.351(6)	F16–C69	1.348(6)
Cu2–N7	2.062(6)	C32–C34	1.429(8)	F10–C60	1.353(6)	C61–C72	1.405(9)
Cu2–N8	2.138(6)	C35–C36	1.400(8)	F11–C57	1.338(6)	C61–C62	1.414(9)
Cu2–N11	2.149(7)	F5–C42	1.337(6)	F12–C58	1.352(6)	C61–C71	1.422(8)
Cu2–N10	2.190(7)	F6–C41	1.343(6)	C49–C50	1.419(9)	C62–N27	1.148(8)
Cu2–N12	2.231(6)	F7–C44	1.335(7)	C49–C59	1.436(8)	C63–N25	1.144(8)
F1–C28	1.348(6)	F8–C46	1.343(6)	C49–C52	1.440(9)	C63–C65	1.422(9)
F2–C31	1.344(6)	C37–N17	1.142(8)	C50–N21	1.146(8)	C64–C70	1.364(8)
F3–C27	1.339(6)	C37–C39	1.431(9)	C51–C60	1.339(8)	C64–C66	1.401(8)
F4–C30	1.354(6)	C38–N20	1.128(7)	C51–C56	1.405(7)	C65–C66	1.408(8)
N13–C25	1.136(7)	C38–C39	1.431(9)	C52–N22	1.138(8)	C65–C68	1.421(10)
N14–C34	1.148(7)	C39–C40	1.418(8)	C53–N24	1.150(7)	C66–C67	1.403(8)
N15–C33	1.134(7)	C40–C41	1.409(8)	C53–C54	1.419(8)	C67–C69	1.353(8)
N16–C26	1.136(8)	C40–C46	1.411(8)	C54–C55	1.420(8)	C68–N26	1.135(9)
C25–C35	1.429(9)	C41–C42	1.361(8)	C54–C56	1.428(7)	C69–C71	1.400(8)
C26–C35	1.426(9)	C42–C43	1.403(8)	C55–N23	1.145(7)	C70–C71	1.417(8)
C27–C28	1.344(8)	C43–C45	1.408(8)	C56–C57	1.410(7)	C72–N28	1.145(8)
N2–Cu1–N3	175.7(2)	N2–Cu1–N6	80.9(2)	N9–Cu2–N10	81.6(3)		
N2–Cu1–N5	97.7(2)	N3–Cu1–N6	99.2(2)	N7–Cu2–N10	98.6(3)		
N3–Cu1–N5	82.4(2)	N5–Cu1–N6	176.6(2)	N8–Cu2–N10	100.6(2)		
N2–Cu1–N1	82.2(2)	N1–Cu1–N6	80.2(2)	N11–Cu2–N10	80.3(3)		
N3–Cu1–N1	93.6(2)	N4–Cu1–N6	96.9(2)	N9–Cu2–N12	100.1(3)		
N5–Cu1–N1	102.7(2)	N9–Cu2–N7	179.1(3)	N7–Cu2–N12	79.8(3)		
N2–Cu1–N4	102.6(2)	N9–Cu2–N8	96.9(3)	N8–Cu2–N12	80.5(2)		
N3–Cu1–N4	81.7(2)	N7–Cu2–N8	82.1(2)	N11–Cu2–N12	98.7(3)		
N5–Cu1–N4	80.4(2)	N7–Cu2–N11	99.9(3)	N10–Cu2–N12	177.9(3)		
N1–Cu1–N4	174.1(2)	N8–Cu2–N11	177.7(3)	N9–Cu2–N11	81.0(3)		

The compounds show semiconducting behavior with room temperature conductivity values of 3.5×10^{-6} and 2×10^{-7} S cm^{-1} and activation energies of 0.11 and 0.30 eV for TCNQ and $TCNQF_4$, respectively.

Optical properties

1 Experimental results

The IR spectra of the powder samples in KBr pellets were recorded on a Nicolet 750 FTIR spectrophotometer. The IR spectra of the TCNQ derivatives offer a convenient diagnosis of the formal oxidation state and the coordinative status of these organic acceptor molecules.[14] Neutral TCNQ shows the following characteristic vibration frequencies: $\nu(C{\equiv}N)=2228$ cm^{-1}, $\nu_{20}(b_{1u})=1530$ cm^{-1}, $\nu_{34}(b_{2u})=1524$ cm^{-1}, $\nu_4(a_g)=1424$ cm^{-1}, $\nu_{50}(b_{3u})=860$ cm^{-1} and $\nu_7(a_g)=705$ cm^{-1}. For the radical anion $TCNQ^{\bullet-}$ these vibrational modes are observed at 2194/2177, 1577, 1507, 1386, 824 and 722 cm^{-1} respectively. In the IR spectra of the bis-derivatives of TCNQ (**1** and **2**), the observed bands at 2176, 2156, 1579, 1501, 1360, 832 and 719 cm^{-1} (**1**) and 2174, 2156, 1578, 1501, 1359, 832 and 719 cm^{-1} (**2**) clearly indicate that all the TCNQ molecules are present in their reduced form.[14,15] The $\nu(C{\equiv}N)$ band pattern shows the characteristic features of $(TCNQ)_2^{2-}$ out of sphere coordination.[9] For $[Cu([9]aneN_3)_2](TCNQ)_3$, the IR spectrum is characteristic of a delocalized mixed valence state with intermediate frequencies between the neutral and ionic molecules of TCNQ. The bands of the a_g modes are broad and are displaced to lower energies owing to electron–molecular vibration coupling. The most characteristic feature is the presence of the charge transfer band as a broad absorption localized around 3400 cm^{-1}. All antiresonances in the parallel polarization may be attributed to the excitation of totally symmetric a_g intramolecular vibrations of TCNQ, which demonstrates that the charge transfer excitation takes place along the stack composed only of TCNQ molecules.[16] The IR spectra in the temperature range 297.5–20 K show at $T<230$ K a weak absorption at 2212 cm^{-1} that can be attributed to a neutral TCNQ:

$$(TCNQ)_3^{2-}\rightarrow(TCNQ)_2^{2-}\text{–}TCNQ^0$$

For derivative **4** the assignment of the absorptions can be made by comparison with $Rb(TCNQF_4)$[17] with assigned bands, $\nu_{18}(b_{1u})=2210$ cm^{-1}, $\nu_{32}(b_{2u})=2190$ cm^{-1}, $\nu_2(a_g)=1630$ cm^{-1}, $\nu_{33}(b_{2u})=1539$ cm^{-1}, $\nu_{19}(b_{1u})=1500$ cm^{-1}, $\nu_3(a_g)=1395$ cm^{-1}, $\nu_{20}(b_{1u})=1351$ cm^{-1}, 1348 cm^{-1}, $\nu_4(a_g)=1262$ cm^{-1}, $\nu_{35}(b_{2u})=1207$ cm^{-1}, $\nu_{21}(b_{1u})=1146$ cm^{-1}, $\nu_{36}(b_{2u})=977$ cm^{-1}, $\nu_5(a_g)=876$ cm^{-1} and $\nu_{37}(b_{3u})=551$ cm^{-1}. For compound **4** these vibrational modes are observed at 2213/2193, 2175, 1635, 1541, 1500, 1399, 1354/1348/1339, 1266, 1208/1196, 1143, 969, 856 and 554 cm^{-1} respectively, clearly indicating that all the $TCNQF_4$ molecules are present in their reduced form.

We note again that the electronic structure of **4** may be described in terms of two electrons per $TCNQF_4$ dimer, because both the positions of the IR bands are the same and the CT band at 6500 cm^{-1} is very close to the CT band at 6400 cm^{-1} in $Rb(TCNQF_4)$, the latter being known to be due to dimerized compound in its low-temperature phase.

Electronic solution and diffuse reflectance spectra were recorded on a Cary 5 spectrophotometer equipped with a praying mantis 3000–200 nm accessory. The solid state electronic spectra of **1** and **2** show absorptions at 8900, 13600, 17800, 25900, 34000 and 39500 cm^{-1}. These bands are broad and intense corresponding to $(TCNQ)_2^{2-}$ dimers and they dominate the spectra. The nickel(II) and copper(II) d→d transitions are less intense and obscured by these bands. The first band centered at 8900 cm^{-1} is broad and results from the intradimer charge transfer transition (CT_1) between radical anions ($TCNQ^{\bullet-}$ $TCNQ^{\bullet-}\rightarrow TCNQ^0$ $TCNQ^{2-}$), usually observed in the 7500–11000 cm^{-1} range.[18] The maxima at 13600, 17800 and 25900 cm^{-1} can be attributed to locally excited levels of the anion radical, corresponding to the usual intramolecular transitions.[19] Finally, the bands at 34000 and

39500 cm^{-1} can be assigned to charge transfer bands involving the polyamine unit.[20,21] Compound **3** shows absorptions at 7700, 13000, 24000, 33000 and 34000 cm^{-1}. The first band is broad and corresponds to the intradimer charge transfer transition (CT_1). The spectrum shows the two locally excited intramolecular transitions at 13000 and 24500 cm^{-1}, respectively. As in compounds **1** and **2** the higher energy bands correspond to the metallomacrocyclic units.

The electronic spectra in acetonitrile solution of compounds **1**–**3** show two absorptions at 11900 and 25400 cm^{-1} corresponding to the LE_1 and LE_2 locally excited levels of the anion radical.[22] The intensity ratio for these two bands is a clear indicator of the oxidation state of the TCNQ groups present in solution, since neutral TCNQ only shows the band at 25400 cm^{-1}. Solutions containing only $TCNQ^-$ show an absorbance ratio of $\varepsilon(25400)/\varepsilon(11900)=0.5$, while this value is higher when both neutral and anionic TCNQ molecules are present. The ratio for compounds **1** and **2** of 0.56 confirms that only $TCNQ^-$ is present, whereas a ratio of 1.18 for **3**, corresponds to one neutral and two anionic species.

2 Theoretical model

The optical properties of a molecular trimer with two π-delocalised electrons have been previously calculated when both central and non-central molecules are symmetric.[23] In this case, only two electronic charge-transfer excitations are allowed: one corresponding to a transition between charged and neutral molecules and the other arising from transition to a final state with two charges on the same molecule. The latter transition originates in the effect of the electronic correlation but has a much smaller intensity and occurs at higher wavenumber than the former transition, so in a discussion concerning the electron–molecular vibration coupling in a trimer with two π-delocalised electrons, the electronic correlations may be disregarded. Consequently, in our model we neglect Coulomb interaction between two electrons and consider the ABA trimer as two independent KLM and MLK trimers constructed from the halves of the TCNQ molecules with one electron on each new trimer in agreement with the structural data. In order to account for the observed asymmetry of the molecule A, the site energies of K and M sites corresponding to different halves of the A molecule are assumed to differ. The electronic Hamiltonian then may be written in a very simple from

$$H_C=\Delta_K n_K+\Delta_M n_M-t(c_K^{+}c_L+c_L^{+}c_M+h.c.) \quad (1)$$

where, as usual, *h.c.* denotes the hermitian conjugate, $c^{+}_i(c_i)$ denotes the creation (annihilation) operator for the electron on the site i, $n_i=c^{+}_i c_i$, t denotes the transfer integral and the site energy of the central fragment L is taken as the energy origin. The eigenvalues of the Hamiltonian (1) are given by the roots of the following cubic equation

$$E^3-(\Delta_K+\Delta_M)E^2+(\Delta_K\Delta_M-2t^2)E+(\Delta_K+\Delta_M)t^2=0 \quad (2)$$

and the eigenfunctions are:

$$|\beta\rangle=(1+\delta_K{}^2+\delta_M{}^2)^{-1/2}(\delta_K c_K{}^{+}+c_L{}^{+}+\delta_M c_M{}^{+})|0\rangle \quad (3)$$

where $\delta_K=t/(\Delta_K-E)$ and $\delta_M=t/(\Delta_M-E)$.

The charge distribution in the KLM trimer is given by the squares of the coefficients in the ground state wavefunction $|1>$ in eqn. (3) and depends on three parameters Δ_K/t, Δ_M/t and E_1/t, where E_1 is the ground state energy. Using the 'experimental' charges as already determined (see X-ray crystal structures), we have three equations for the three unknown parameters (Δ_K/t), (Δ_M/t) and (E_1/t), and can obtain all the eigenvalues and eigenfunctions of the Hamiltonian (1):

$$\begin{aligned}
&E_1=-1.725t,\ |1\rangle=(0.500c_K{}^{+}+0.633c_L{}^{+}+0.591c_M{}^{+})|0\rangle;\\
&E_2=-0.555t,\ |2\rangle=(0.723c_K{}^{+}+0.069c_L{}^{+}-0.687c_M{}^{+})|0\rangle;\\
&E_3=+1.165t,\ |3\rangle=(0.475c_K{}^{+}-0.771c_L{}^{+}+0.424c_M{}^{+})|0\rangle
\end{aligned} \quad (4)$$

For calculations of the absorption spectra we shall consider the Hamiltonian which includes electron–molecular vibration (EMV) coupling and interaction with the external electric field in the form:[23]

$$H=H_e+\sum_{i,\alpha}\frac{\omega_{\alpha i}}{4}(\Pi_{\alpha i}{}^2+Q_{\alpha i}{}^2)+\sum_{i,\alpha}g_\alpha Q_{\alpha i}n_i-\vec{p}\vec{F} \quad (5)$$

where the second term describes the totally symmetric intramolecular vibrations; $\Pi_{\alpha i}$ is the canonically conjugated

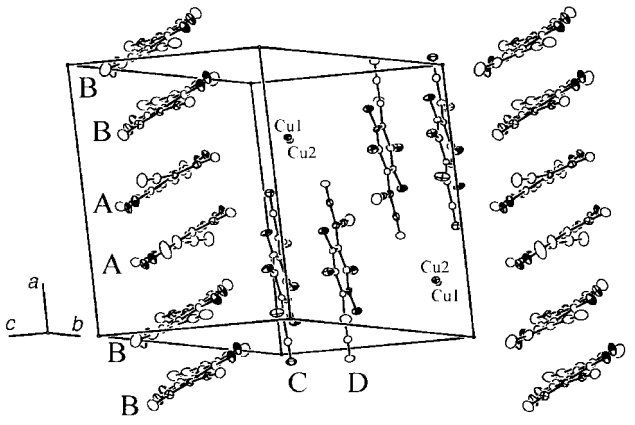

Fig. 7 Stacking of the $(TCNQF_4)_2{}^{2-}$ dimers in $[Cu([9]aneN_3)_2](TCNQF_4)_2$ **4**.

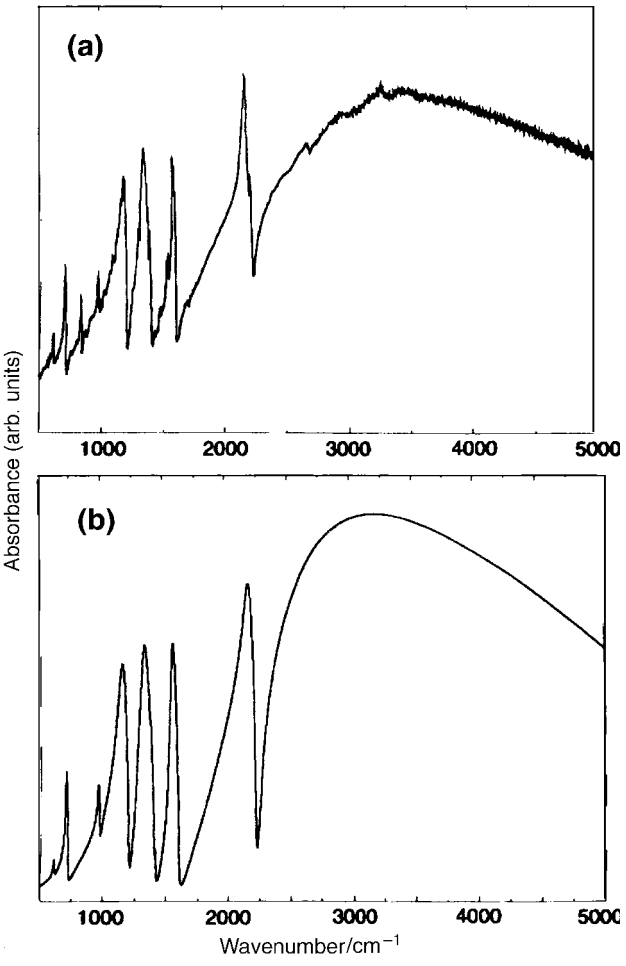

Fig. 8 Experimental absorption spectrum of powdered $[Cu([9]aneN_3)](TCNQ)_3$ **3** at room temperature in the range 500–5000 cm^{-1} (a) and the calculated spectrum (b).

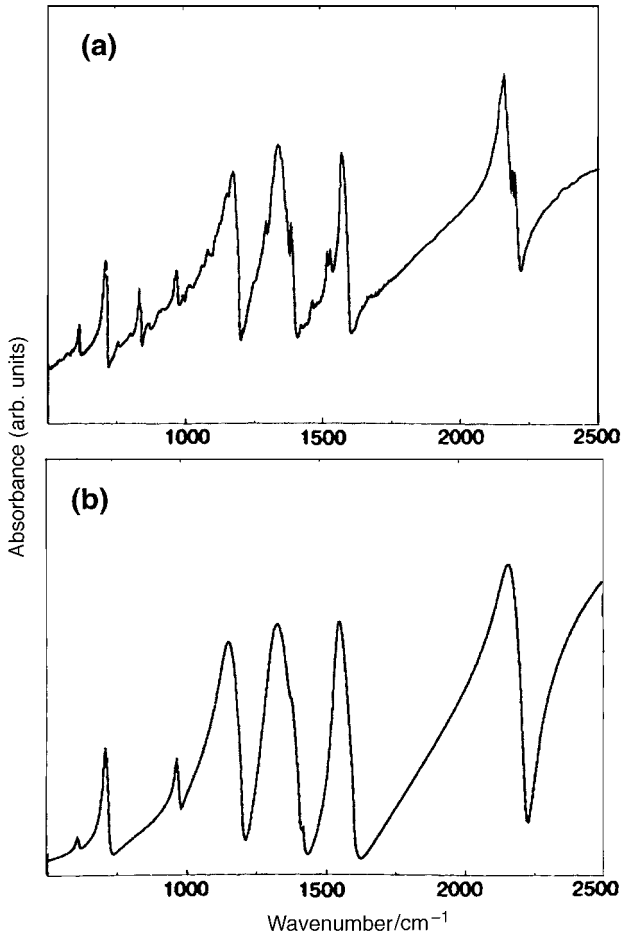

Fig. 9 Experimental IR absorbance of [Cu([9]aneN$_3$)](TCNQ)$_3$ **3** at room temperature in the range 500–2500 cm^{-1} (a) and calculated absorbance (b).

momentum for the dimensionless coordinate $Q_{\alpha i}$ of the αth mode of vibration with the frequency $\omega_{\alpha i}$ of the site designated by i. The strength of EMV coupling is defined by the coupling constant g_α in the third term and finally $\vec{p}$ denotes the electric dipole moment induced in the molecular cluster by the externally applied field $\vec{F}$.

The optical characteristics may be calculated using the general formulae for the cluster model[23] and the result for absorbance is shown in Fig. 8 and 9. The molecular frequencies were found using the 'experimental' values of site charges and assuming a linear dependence on charge between the known values for neutral TCNQ[24] and its singly charged ion.[14] The EMV coupling constants g_α are molecular characteristics,[25] so the only fitting parameter required is the transfer integral t which is found to be 0.25 eV. This value is quite typical for TCNQ charge-transfer salts.[23]

Magnetic properties

Magnetic measurements were made on polycrystalline samples using a SQUID MPMS-5S magnetometer manufactured by Quantum Design, in the temperature range 1.7–300 K, with a magnetic field strength up to 50 kG (5 T). The experimental data were corrected for atomic diamagnetism from known Pascal constants.

The bulk static magnetic susceptibility has been measured over the temperature range 1.7–300 K. Compound **1** presents a magnetic behavior variation typical of non-interacting octahedral nickel(II) ions and the molar magnetic susceptibility data have been fitted with the zero field splitting equation

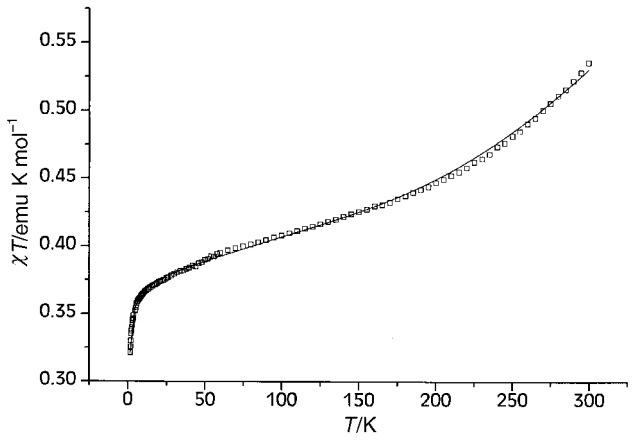

Fig. 10 Temperature dependence of χT for [Cu([9]aneN3)$_2$](TCNQ)$_3$ **4**. The solid line represents the fit of the data as discussed in the text.

[eqn. (6)].[26]

$$\chi=\frac{2Ng^2\mu_B{}^2}{3kT}\left[\frac{(2/x)-[2\exp(-x)/x]+\exp(-x)}{1+2\exp(-x)}\right] \quad (6)$$

where, $x=D/kT$ and N, g, μ_B and k denote respectively Avogadro's number, the g-factor value of nickel, the Bohr magneton and the Boltzman constant; D is the zero field splitting of Ni^{II} in cm^{-1}. The best fit to eqn. (6) was obtained with $g=2.03(1)$ and $D=-9.88(1)$ cm^{-1}.

Compounds **2** and **4** present a magnetic susceptibility temperature dependence typical for copper(II) compounds. The susceptibility values follow the Curie–Weiss law, with the same Curie constant value $C=0.40$ emu K mol^{-1} and a Weiss temperature of $\theta=-2.16(1)$ and $-0.23(1)$ K, respectively. The observed Curie constant value corresponds to an effective magnetic moment of 1.79 μ_B and may be attributed to copper(II) $S=1/2$ with a g-factor value of 2.05. The experimental values of χT for **3** steadily decrease from 0.405 emu K mol^{-1} at 300 K to 0.365 emu K mol^{-1} at 70 K, where an inflection point is observed. Such behavior indicates that in the high temperature region there is a small contribution from the dimers to the magnetic susceptibility, Fig. 10. Below 70 K, the values of χT decrease more rapidly down to 0.32 emu K mol^{-1} at 1.8 K. The molar magnetic susceptibility data were fitted by the sum of the Curie and Bleaney–Bowers equations in the temperature range $40<T<250$ K.[27]

$$\chi_{tot}=\frac{Ng_{Cu}{}^2\mu_B{}^2}{4k_BT}+\frac{Ng^2\mu_B{}^2}{k_BT}\left[\frac{2}{3+\exp(-2J/k_BT)}\right] \quad (7)$$

Here g_{Cu}, g and J denote the g value of copper, the g value of TCNQ and the exchange coupling constant for interacting TCNQ pairs. In order to reduce the number of parameters, a value of $g=2.00$ has been kept fixed in the fitting process. The best fit to eqn. (7) has been obtained with $J=-417(1)$ cm^{-1} for the singlet–triplet energy, this result shows the existence of an excited triplet state as in other TCNQ salts.[28] The fitting process may then be extended to the entire temperature range, and if the Curie term is substituted by the Curie–Weiss law in eqn. (7) keeping the other parameters fixed at the fitted values given above, we obtain a value of $\theta=-0.32(1)$ K, indicating the presence of very small antiferromagnetic interactions between the Cu^{2+} ions.

The single crystal and powder EPR spectra were measured with a Bruker ESP 300E apparatus equipped with a Bruker ER035M gaussmeter and an Oxford JTC4 cryostat. Room temperature powder EPR spectra of the copper derivatives were obtained. The value of the g-factor for **2** and **4** ($g=2.11$) is attributed to the Cu^{2+} ion. Compound **3** has also been studied by EPR on single crystals and we have measured the

angular dependence of the EPR *g*-factor. The single crystal EPR spectra show only one signal attributable to the Cu^{2+} ion. The *g*-factor components, which are obtained from the angular dependencies of the EPR signal are $g_{max} = 2.16$, $g_{med} = 2.10$ and $g_{min} = 2.06$. These values are similar to those found at low temperature for $[Cu([9]aneN_3)_2][Cu(CN)_3]\cdot 2H_2O$ where the environment of the Cu^{2+} centre exhibits a dynamic Jahn–Teller effect with a maximum effect at low temperature.[12] These results confirm the static magnetic measurements, where the strong influence of the transition metals is evidenced.

Summary

Four new salts of $[M([9]aneN_3)_2]^{2+}$ ($M = Ni^{II}$ or Cu^{II}) with TCNQ and $TCNQF_4$ have been synthesized: $[Ni([9]aneN_3)_2](TCNQ)_2$ **1**, $[Cu([9]aneN_3)_2](TCNQ)_2$ **2**, $[Cu([9]aneN_3)_2](TCNQ)_3$ **3** and $[Cu([9]aneN_3)_2](TCNQF_4)_2$ **4**. Compounds **1** and **2** are isostructural, with alternated metallic fragments and $(TCNQ)_2^{2-}$ dimers in the three spatial directions, whereas compound **4** shows a more complex structure built by $(TCNQF_4)_2^{2-}$ units forming linear chains. Compounds **1** and **2** behave as insulators, whereas compound **4** shows semiconducting behavior with an activation energy of 0.30 eV. Their magnetic behavior corresponds to the contribution coming from the metallic fragments.

A higher electronic delocalization is present in compound **3** built by trimeric $(TCNQ)_3^{2-}$ units and $[Cu([9]aneN_3)_2]^{2+}$ fragments forming segregated stacks. This compound behaves as a semiconductor with an activation energy of 0.11 eV and the magnetic behavior is interpreted as arising from two independent contributions corresponding to Cu^{2+} and organic radicals.

Finally the optical properties are in accord with the distribution of electronic density in the organic systems, a theoretical model of an asymmetrical molecular trimer with two π-delocalised electrons has been proposed to interpret the optical measurements which include in particular the characteristic a_g vibrational bands due to electron–intramolecular vibration coupling inside the TCNQ stacks.

Acknowledgements

We gratefully acknowledge the D.G.E.S. for financial support, projects PB94–0240 and PB97–0236, and the UE for a Marie Curie Research Training Grant. One of us (M.T.A.) thanks the Universidad San Pablo-C.E.U. for the facilities given during her stay in Bordeaux.

References

1 M. Kurmoo, A. W. Graham, P. Day, S. J. Coles, M. B. Hursthouse, J. L. Caulfield, J. Singleton, F. L. Pratt, W. Hayes, L. Ducasse and P. Guionneau, *J. Am. Chem. Soc.*, 1995, **117**, 12209.
2 W. Kaim and M. Moscherosch, *Coord. Chem. Rev.*, 1994, **129**, 157; H. Zhao, R. A. Heintz, K. R. Dunbar and R. D. Rogers, *J. Am. Chem. Soc.*, 1996, **118**, 12844.
3 M. C. Grossel, *Chem. Mater.*, 1996, **8**, 977; L. J. Pace, A. Ulman and J. A. Ibers, *Inorg. Chem.*, 1982, **21**, 199.
4 H. Endres, in *Extended Linear Chain Compounds*, ed. J. S. Miller, Plenum, New York, 1982, ch. 3, p. 263; L. Ballester, A. Gutiérrez, M. F. Perpiñán, U. Amador, M. T. Azcondo, A. E. Sánchez-Peláez and C. Bellitto, *Inorg. Chem.*, 1997, **36**, 639.
5 L. Ballester, M. C. Barral, A. Gutiérrez, R. Jiménez-Aparicio, J. M. Martínez-Muyo, M. F. Perpiñán, M. A. Monge and C. Ruiz-Valero, *J. Chem. Soc., Chem. Commun.*, 1991, 1396.
6 L. Ballester, A. Gutiérrez, M. F. Perpiñán, M. T. Azcondo, A. E. Sánchez-Peláez and U. Amador, *Anal. Quim. Int. Ed.*, 1996, **92**, 275.
7 L. Ballester, A. M. Gil, A. Gutiérrez, M. F. Perpiñán, M. T. Azcondo, A. E. Sánchez-Peláez, U. Amador, J. Campo and F. Palacio, *Inorg. Chem.*, 1997, **36**, 5291.
8 X. Wang, L. M. Liable-Sands, J. L. Manson, A. L. Rheingold and J. S. Miller, *Chem. Commun.*, 1996, 1979.
9 L. R. Melby, R. J. Herder, W. Mahler, R. E. Benson and W. E. Mochel, *J. Am. Chem. Soc.*, 1962, **84**, 3374.
10 R. Yang and L. J. Zompa, *Inorg. Chem.*, 1976, **15**, 1499.
11 M. G. Nardelli, G. V. Gasparri, A. Musatti and A. Manfredotti, *Acta Crystallogr.*, 1966, **21**, 910.
12 P. Chaudhuri, K. Oder, K. Wieghardt, J. Weiss, J. Reedijk, W. Hinrichs, J. Wood, A. Ozarowsky, H. Stratemaier and D. Reinen, *Inorg. Chem.*, 1986, **25**, 2951.
13 S. Flandrois and D. Chasseau, *Acta Crystallogr., Sect. B*, 1977, **33**, 2744.
14 R. Bozio, A. Girlando and C. Pecile, *J. Chem. Soc., Faraday Trans.*, 1975, **71**, 1237.
15 R. Bozio, I. Zanon, A. Girlando and C. Pecile, *J. Chem. Soc., Faraday Trans.*, 1978, **74**, 235.
16 J. Ramos, V. M. Yartsev, S. Golhen, L. Ouahab and P. Delhaes, *J. Mater. Chem.*, 1997, **7**, 1313.
17 M. Meneghetti, A. Girlando and C. Pecile, *J. Chem. Phys.*, 1985, **83**, 3134.
18 J. B. Torrance, *Acc. Chem. Res.*, 1979, **12**, 79.
19 M. Schwartz and W. E. Hatfield, *Inorg. Chem.*, 1987, **26**, 2823.
20 A. R. Amudsen, J. Whelon and B. Bosnich, *J. Am. Chem. Soc.*, 1977, **99**, 6730.
21 A. B. Lever, *Inorganic Electronic Spectroscopy*, Elsevier, Amsterdam, 1984, p. 356.
22 Y. Iida, *Bull. Chem. Soc. Jpn.*, 1969, **42**, 673.
23 V. M. Yartsev, *Phys. Status Solidi B*, 1982, **112**, 279.
24 M. Futamata, Y. Morioka and I. Nakagawa, *Spectrochim. Acta, Part A*, 1983, **39**, 515.
25 M. J. Rice, V. M. Yartsev and C. S. Jacobsen, *Phys. Rev. B*, 1980, **21**, 3437.
26 R. L. Carlin, *Magnetochemistry*, Springer-Verlag, Berlin, Heidelberg, 1986, p. 24.
27 B. Bleaney and K. D. Bowers, *Proc. R. Soc. London, Ser. A*, 1952, **214**, 451.
28 J. Krzystek and J. U. Von Schutz, *Adv. Chem. Phys.*, 1992, **86**, 167.

Paper 8/07595F